Molecular Neurobiology (2019) 56:1437–1450
https://doi.org/10.1007/s12035-018-1144-3

Sustained CaMKII Delta Gene Expression Is Specifically Required for Long-Lasting Memories in Mice

Gisela Zalcman[1,2] · Noel Federman[3] · Ana Fiszbein[2] · Verónica de la Fuente[1,2] · Leila Ameneiro[1,2] · Ignacio Schor[2] · Arturo Romano[1,2]

Received: 29 January 2018 / Accepted: 22 May 2018 / Published online: 9 June 2018

Abstract

Although important information is available on the molecular mechanisms of long-term memory formation, little is known about the processes underlying memory persistence in the brain. Here, we report that persistent gene expression of CaMKIIδ isoform participates in object recognition long-lasting memory storage in mice hippocampus. We found that CaMKIIδ mRNA expression was sustained up to one week after training and paralleled memory retention. Antisense DNA infusion in the hippocampus during consolidation or even after consolidation impairs 7-day- but not 1-day-long memory, supporting a role of CaMKIIδ in memory persistence. CaMKIIδ gene expression was accompanied by long-lasting nucleosome occupancy changes at its promoter. This epigenetic mechanism is described for the first time in a memory process and offers a novel mechanism for persistent gene expression in neurons. CaMKIIδ protein is mainly present in nucleus and presynaptic terminals, suggesting a role in these subcellular compartments for memory persistence. All these results point to a key function of the sustained gene expression of this overlooked CaMKII isoform in long-lasting memories.

Keywords CaMKII · Long-term memory · Hippocampus · Neuroepigenetics · Nucleosome occupancy

Introduction

A considerable body of data in the last decades has provided important information on the molecular basis of memory formation. However, the understanding of how memories persist and are maintained over time is still relatively scarce. Neuroepigenetic mechanisms that regulate gene expression have been proposed to be involved in memory storage [1]. DNA methylation was found to participate in remote memory maintenance during system consolidation [2]. In addition, specific epigenetic mechanisms are activated during consolidation which makes some memories more persistent than others, as we recently described for histone acetylation in mice hippocampus [3]. Also, the protein kinase PKMz has been proposed, although with uncertainties, as a specific mechanism of long-term memory (LTM) maintenance in both vertebrates and invertebrates [4, 5].

Ca^{2+}/calmodulin-dependent protein kinase II (CaMKII) has four isoforms, α, β, γ, and δ, derived from four different but closely related genes [6]. All CaMKII enzymes are activated by the Ca^{+2}/calmodulin (CaM) complex that is formed after Ca^{2+} entrance upon neuronal activity. CaMKII activity increases during LTM formation, and inhibition of its activity has a negative effect on this process [7, 8]. Studies in CaMKII α and β mutant mice showed that both are necessary for LTM formation [9, 10]. In contrast, few data are available for δ isoform in the nervous system. The first evidences linking this gene with memory are the following: a work showing an

Gisela Zalcman and Noel Federman contributed equally to this work.

Electronic supplementary material The online version of this article (https://doi.org/10.1007/s12035-018-1144-3) contains supplementary material, which is available to authorized users.

✉ Noel Federman
nfederman@ibioba-mpsp-conicet.gov.ar

[1] Laboratorio de Neurobiología de la Memoria, Departamento de Fisiología, Biología Molecular y Celular, Facultad de Ciencias Exactas y Naturales, Universidad de Buenos Aires, Buenos Aires, Argentina

[2] Instituto de Fisiología, Biología Molecular y Neurociencias (IFIByNE), UBA-CONICET, Ciudad Universitaria, 1428EHA Buenos Aires, Argentina

[3] Laboratorio de Circuitos Neuronales, Instituto de Investigación en Biomedicina de Buenos Aires (IBioBA)—CONICET—Partner Institute of the Max Planck Society, Godoy Cruz 2390, C1425FQD Buenos Aires, Argentina

increase in its expression 6 h after trace fear conditioning [11] and a recent report from our group in which we show that its gene expression is induced during object recognition memory-consolidation only in persistent memories [3].

Considering that epigenetic modifications are potentially stable, some of them lasting throughout the life of a cell, they are good candidates to mediate neuronal plasticity during memory consolidation and maintenance [1]. Memory-related epigenetic mechanisms studied so far have been mainly focused on post-translational histone modification [12], deposition of histone variants [13, 14], and DNA methylation [2]. Histone octamer associates with DNA to form the nucleosome, the building block of chromatin. Recent reports have highlighted the importance of a neuronal chromosome remodeling complex, the nBAF complex, in different memory processes and, in particular, in object recognition memory [15–18]. These complexes can cause nucleosome sliding, eviction, or histone variant exchange that can in turn introduce modifications in nucleosome occupancy at particular DNA sequences, which could also participate in the regulation of gene expression [19]. However, it is not known if nucleosome occupancy changes take place indeed during memory storage and which would be its role in this process.

In the present work, we studied CaMKIIδ gene expression profile over time, its requirement in persistence and maintenance of long-lasting memories, and the changes at nucleosome occupancy level in its promoter, as a new epigenetic mechanism related to its sustained expression during memory persistence. In addition, we described the cellular distribution of the protein, which could help to disclose a differential role for this CaMKII isoform in neurons. Altogether, our data support a key role for CaMKIIδ in the persistence of enduring memories.

Results

Expression of Camk2d Is Associated with Memory Retention

In novel object recognition task (NOR), memory is evaluated by the differences in the exploration time of novel and familiar objects. Figure 1a shows a description of the configuration of the objects in the training and testing sessions employed in this work. We performed a training session of 10 min (standard training protocol, TR) or 15 min (strong training protocol, sTR) and assessed memory retention 1, 7, or 20 days after (independent experiments). We also included a control group (No-TR) which in the training session was placed inside the experimental arena but without objects (Fig. 1b). The object exploration time for the animals that received a strong training is significantly higher than for those that were trained with the standard protocol (sTR (15 min) = 17.2 ± 0.9 s, TR (10 min) = 13.3 ± 0.9 s, $p = 0.0229$). In the testing session, significantly enhanced discrimination index (DI%) was found for TR and sTR groups with respect to No-TR group after 1 day (Fig. 1c, 1 day), indicating similar LTM formation after both types of training. In the 7-day test, memory retention was significantly higher than non-trained animals only for the sTR group (Fig. 1c, 7 days), indicating that a strong training protocol induces a more lasting memory than the standard protocol. Finally, when memory was tested 20 days after strong training, no significant retention between groups was found (Fig. 1c, 20 days).

Next, we studied the temporal profile of *camk2d* gene expression in both training conditions for the different timepoints studied before. Total RNA was extracted from the hippocampus 1, 7, or 20 days after training, and qPCR was performed to determine the levels of CaMKIIδ mRNA relative to the No-TR group (Fig. 1d). Significantly higher mRNA levels were found both for TR and sTR groups with respect to the No-TR group, 1 day after training (Fig. 1e, 1 day). Notably, when hippocampal RNA was extracted 7 days after training, significant levels of CaMKIIδ gene expression were found for the sTR group, but no significant differences were found for the TR group vs. No-TR group (Fig. 1e, 7 days) although a tendency for higher levels is observed. In the last experiment, RNA was extracted 20 days after training. No significant differences were found between the No-TR and sTR groups (Fig. 1e, 20 days), indicating that CaMKIIδ mRNA returns to basal levels after 20 days. Interestingly, the results of Fig. 1e show a striking correlation with the behavioral results of Fig. 1c (Fig. 1e inset, $r_{pearson} = 0.9437$, $p = 0.0004$).

The general conclusion of the results of these two experiments is that CaMKIIδ mRNA has a sustained increase after training that showed a tight association with memory retention, being present up to 7 days after strong training and decaying 20 days after.

CaMKII δ Gene Expression Is Necessary for the Formation of Persistent Long-Term Memories

Since the δ isoform of CaMKII had not been studied before in memory-related processes, we decided to investigate if its expression after NOR training was necessary for LTM. To this aim, we developed an oligodeoxynucleotide (ODN) antisense to a CaMKIIδ mRNA fragment (ASO) to induce mRNA knock-down. An ODN with a scrambled sequence (Scrl) was designed to be used as control. A first experiment was carried out to verify that this newly developed ASO could effectively knock-down CaMKIIδ mRNA. The results are shown in Supplementary Fig. 1 and reveal that intrahippocampal infusion of ASO significantly decreases CaMKIIδ mRNA levels compared to Scrl oligonucleotide administration. Therefore, these ODN were further used to

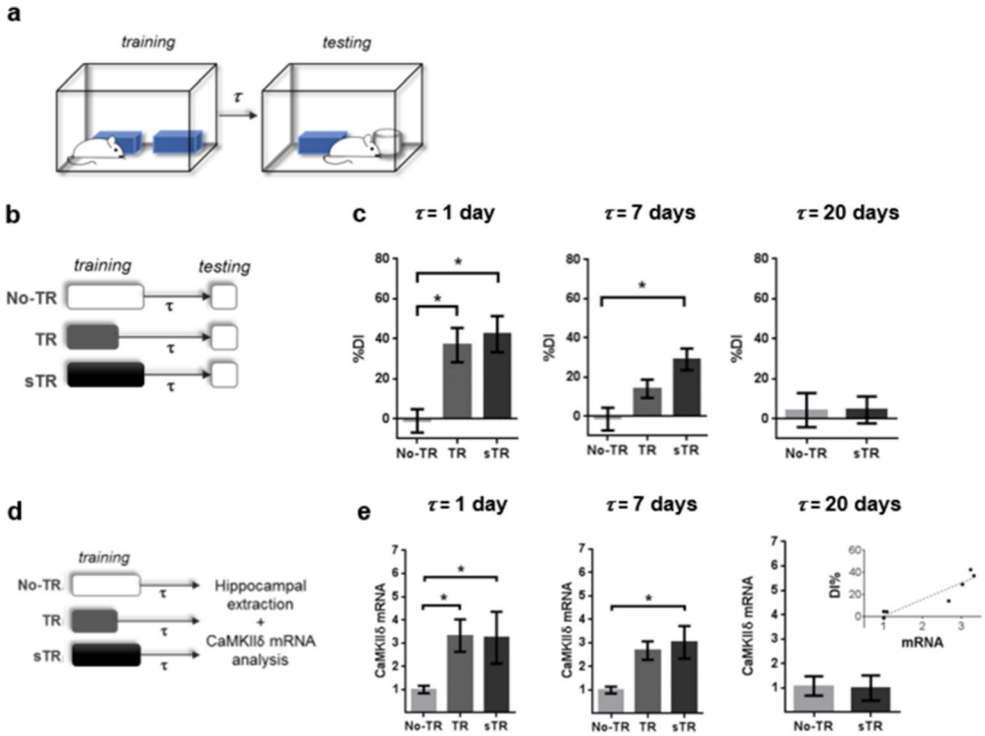

Fig. 1 NOR performance and CaMKIIδ mRNA expression 1, 7, and 20 days after training. (**a**) Experimental design of NOR training and testing sessions. During the training session, animals are allowed to explore two identical objects. At different time points after training (τ), animals are placed again in the experimental arena containing a copy of the previously explored object and a novel object. Animals approach frequently and spend more time exploring the novel than the familiar one. (**b**) Behavioral protocol: No-TR group was exposed to the chamber without objects, TR and sTR groups were exposed to the chamber with two identical objects for 10 or 15 min, respectively. (**c**) %Discrimination Index, %DI 1, 7, and 20 days after training (1 day: $n_{\text{No-TR}} = 8$, $n_{\text{TR}} = 9$, $n_{\text{sTR}} = 9$, $F = 9.31$, $p = 0.0011$; 7 days: $n_{\text{No-TR}} = 9$, $n_{\text{TR}} = 8$, $n_{\text{sTR}} = 9$, $F = 8.19$, $p = 0.0021$; 20 days: $n_{\text{No-TR}} = 9$, $n_{\text{sTR}} = 9$, $t_{16,\ 0.05} = 0.01625$, $p = 0.9872$). (**d**) Behavioral protocol. (**e**) mRNA levels for No-TR, TR, and sTR groups 1, 7, and 20 days after training relative to No-TR (1 day: $n_{\text{No-TR}} = 7$, $n_{\text{TR}} = 7$, $n_{\text{sTR}} = 5$, $F = 3.97$, $p = 0.0399$; 7 days: $n_{\text{No-TR}} = 4$, $n_{\text{TR}} = 5$, $n_{\text{sTR}} = 5$, $F = 4.15$, $p = 0.0454$; 20 days: $n_{\text{No-TR}} = 8$, $n_{\text{sTR}} = 10$, $t_{16,\ 0.05} = 0.1178$, $p = 0.9077$). Inset, correlation between CaMKIIδ mRNA and DI%

evaluate the effect of CaMKIIδ mRNA knock-down on memory retention.

We first studied the role of CaMKIIδ mRNA expression in memory consolidation, which takes place within the first hours after training [20]. We trained two groups of mice with strong training protocol and 2 h after training animals received an injection in each dorsal hippocampus of either ASO or Scrl (Fig. 2a). Twenty-four hours after training, both groups were tested, and no significant differences in the DI% were found (Fig. 2b). Next, we carried out a similar experiment, but the mice were tested 7 days after training. Significantly lower levels of discrimination index were found in the ASO-injected group (Fig. 2c). Notably, total exploration time was not affected by drug treatment in any of the experiments ($TS_{1\ day}$ Scrl = 5.8 s ± 0.4 s; ASO = 5.7 s ± 0.5 s; no statistical significance, $TS_{7\ days}$ Scrl = 4.4 s ± 0.5 s, ASO = 3.6 s ± 0.4 s; no statistical significance), indicating that ASO infusion had no effect on locomotor activity or motivation to explore the objects. Altogether, these experiments show that CaMKIIδ mRNA knock-down in hippocampus during consolidation does not impair LTM formation but impairs its persistence 7 days after. Thus, they support a specific action of CaMKIIδ in the formation of persistent memories.

The finding that CaMKIIδ gene expression can be sustained several days after training and that it parallels memory retention (Fig. 1) encouraged us to test the hypothesis that CaMKIIδ gene expression is necessary for memory to persist on time. For this, we trained two groups of mice with strong training and 1 day after, once memory is considered to have consolidated, animals received intra-hippocampal infusion of either ASO or Scrl and were tested 7 days after training (Fig. 2d). ASO group showed a significant lower level of retention than Scrl group indicating an amnesic effect of the mRNA knock-down and an action of CaMKIIδ gene expression beyond the time window of synaptic consolidation (Fig. 2e).

Strong Training Induces Long-Lasting Nucleosome Occupancy Changes at Camk2d Promoter

Epigenetic mechanisms like histone acetylation and methylation are known to be involved in LTM, but these appear to be transient processes. In search of a more long-lasting chromatin remodeling process that could be involved in the persistence of CaMKIIδ expression, we assessed changes in nucleosome positioning at both the NF-κB-regulated site (κB site) and the

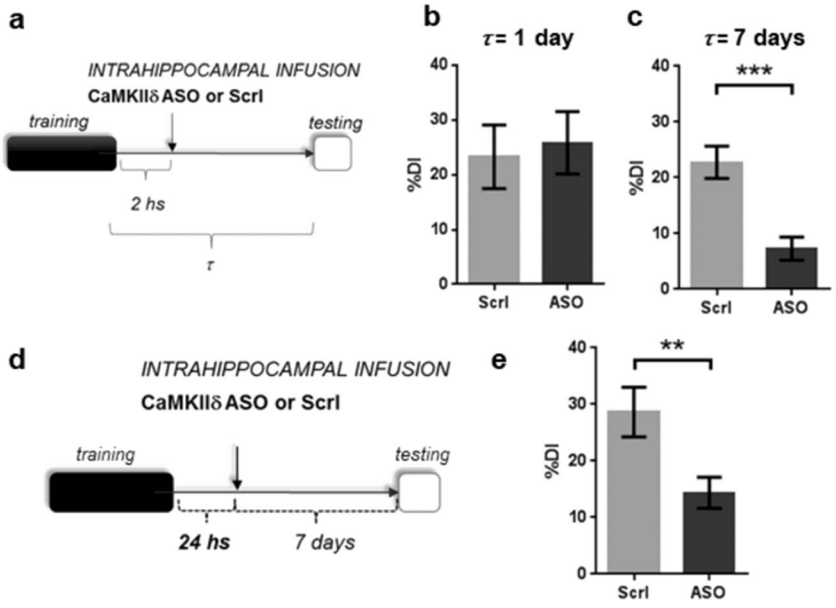

Fig. 2 CaMKIIδ gene expression is specifically required for long-lasting memories. (**a**) Experimental design. (**b**) %DI of Scrl and ASO groups tested 1 day after training ($n_{Scrl} = 9$, $n_{ASO} = 11$, $t_{18,\ 0.05} = 0.3094$, $p = 0.7606$). (**c**) %DI of Scrl and ASO groups, respectively ($n_{Scrl} = 7$, $n_{ASO} = 10$, $t_{15,\ 0.05} = 4.472$, $p = 0.0004$) when tested 7 days after training. *$p < 0.05$, ***$p < 0.0005$. (**d**) Experimental design. (**e**) %DI of Scrl and ASO groups ($n_{No\text{-}TR} = 10$, $n_{sTR} = 14$, $t_{12,\ 0.05} = 2.903$, $p = 0.0082$) when tested 7 days after training. *$p < 0.05$, **$p < 0.005$

transcription start site (TSS) of *camk2d* promoter (Fig. 3a). We chose the κB site because previous evidence showed that NF-κB is bound to CaMKIIδ promoter after experience-dependent induction of gene expression [3, 21]. The TSS site was chosen because changes in nucleosome occupancy on this region are known to regulate the expression of the downstream gene [19, 22, 23]. We studied nucleosome occupancy at these sites at four different time points: 1 h, 3 h, 7 days, and 20 days. The shorter time points were chosen because previous evidence from our lab showed that there is an increase of histone acetylation on *camk2d* promoter 1 h after training and an increase of CaMKIIδ mRNA 3 h after [3]. The others are the time points we used to trace CaMKIIδ mRNA levels (Fig. 1e).

We measured nucleosome occupancy in hippocampal neurons of two groups of animals, No-TR and sTR, at the indicated times after training (Fig. 3b). While no differences were found at the TSS 1 h after training, nucleosome occupancy was significantly reduced in the sTR group with respect to the No-TR group 3 h after training. Conversely, 7 days after training, nucleosomal occupancy was significantly increased, and the differences vanished 20 days after training (Fig. 3c). This picture differs from that observed at the κB site, where we only detected a significant increase in nucleosomal occupancy 3 h after training, which was already abolished at 7 days (Fig. 3d). In contrast, κB sites on NMDA and AMPA receptor gene promoters [24, 25] showed no significant changes in nucleosome occupancy 3 h after training (Fig. 3e,f), suggesting that the observed changes are specific of the *camk2d* promoter.

Our results show opposite changes in nucleosome occupancy at 3 h and 7 days after training; thus, a similar effect on mRNA expression would be expected. However, our evidence indicates that CaMKIIδ mRNA is increased at both time points (Fig. 1e, 7 days) [3]. In order to have a better estimation of *camk2d* gene expression, we decided to measure its pre-mRNA levels at 3 h and 7 days after training. Strikingly, we found a two-fold increase in CaMKIIδ pre-mRNA expression 3 h after training compared to 7 days, indicating that the expression of CaMKIIδ pre-mRNA peaks 3 h after training (Fig. 4a). These results suggest that the decrease in nucleosome occupancy at TSS 3 h after training could facilitate *camk2d* expression while the increase, found 7 days after, could inhibit it.

Finally, we analyzed if a standard training could also induce changes in nucleosome occupancy as those found at 3 h after strong training. To this aim, we performed a similar experiment than in Fig. 3, but the animals were trained with a standard protocol (10 min). We found no significant differences on nucleosome occupancy in the transcription start site or in the κB site (Fig. 4b). Thus, the changes in nucleosome occupancy at the *Camk2d* promoter observed during consolidation take place specifically for long-lasting memories.

Overall, these results indicate that changes in nucleosomal positioning take place at *Camk2d* core promoter and accompany long-lasting CaMKIIδ gene expression.

CaMKIIδ Protein Is Predominantly Present in Nuclei, Dendrites, and Pre-Synaptic Terminals

The cellular distribution of all CaMKII isoforms is a critical determinant of their function, particularly in memory-related processes [26–29]. However, until now, the cellular distribution of neuronal CaMKIIδ protein had not been well described. We performed immunofluorescence studies on coronal brain slices of non-trained mice to characterize, for the first time, CaMKIIδ location in hippocampal neurons. We found CaMKIIδ immunolabeling in hippocampal CA1, CA2, and

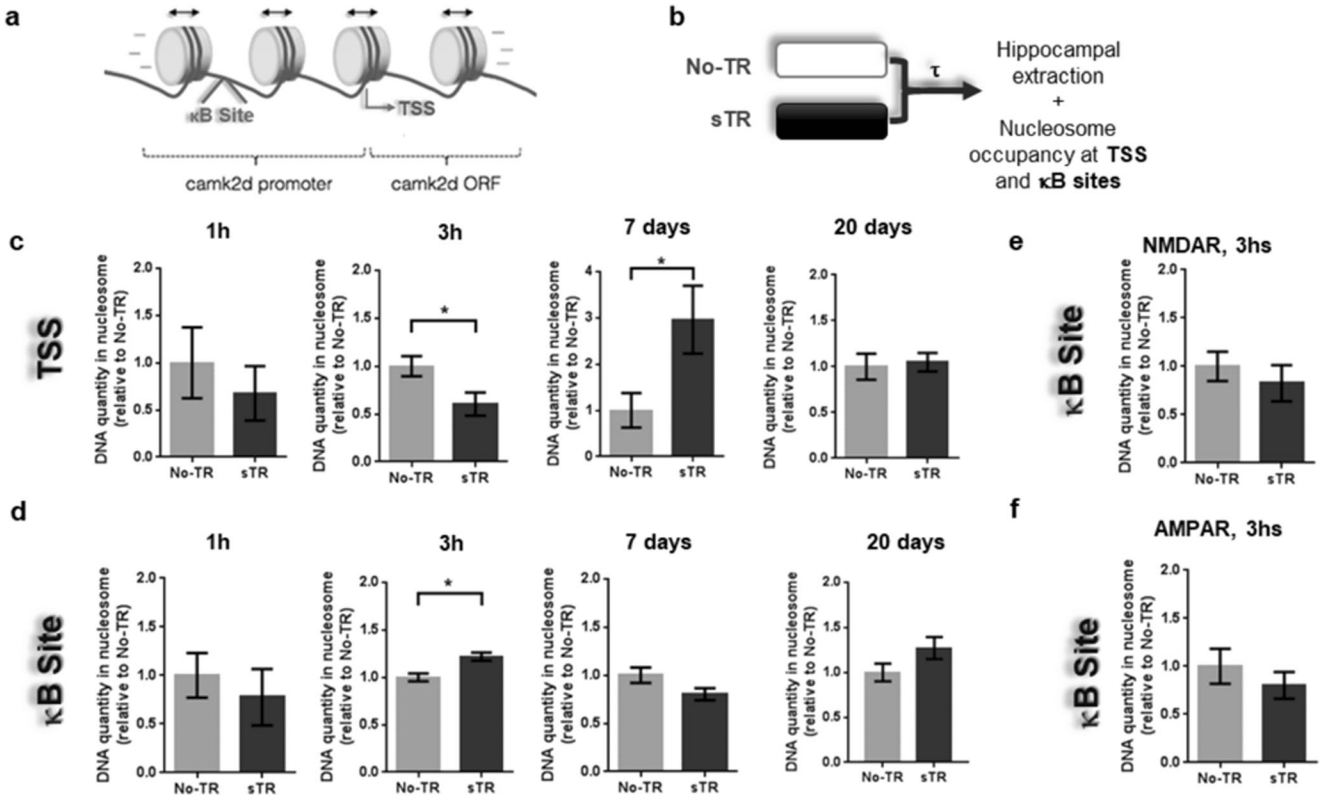

Fig. 3 Nucleosome occupancy at CaMKIIδ κB and TSS sites 1 h, 3 h, 7 days, and 20 days after NOR training. (**a**) Schematic drawing of CaMKIIδ gene showing κB and TSS sites and nucleosomes. ORF, open-reading frame. (**b**) Experimental protocol. (**c**, **d**) TSS (**c**) or κB (**d**) DNA quantity in nucleosomes during and several days after consolidation. In all cases, values are expressed relative to No-TR (TSS 1 h: $n_{\text{No-TR}} = 3$, $n_{\text{sTR}} = 5$, $t_{6,\ 0.05} = 0.6826$, $p =$ ns; TSS 3 h: $n_{\text{No-TR}} = 7$, $n_{\text{sTR}} = 7$, $t_{12,\ 0.05} = 2.459$, $p = 0.0301$; TSS 7 days: $n_{\text{No-TR}} = 5$, $n_{\text{sTR}} = 5$, $t_{8,\ 0.05} = 2.528$, $p = 0.0354$; TSS 20 days: $n_{\text{No-TR}} = 6$, $n_{\text{sTR}} = 8$, $t_{12,\ 0.05} = 0.2952$, $p = 0.7729$) (κB 1 h: $n_{\text{No-TR}} = 4$, $n_{\text{sTR}} = 4$, $t_{6,\ 0.05} = 0.6070$, $p =$ ns; κB 3 h: $n_{\text{No-TR}} = 9$, $n_{\text{sTR}} = 7$, $t_{14,\ 0.05} = 3.655$, $p = 0.0027$; κB 7 days: $n_{\text{No-TR}} = 5$, $n_{\text{sTR}} = 5$, $t_{8,\ 0.05} = 1.926$, $p =$ ns; κB 20 days: $n_{\text{No-TR}} = 5$, $n_{\text{sTR}} = 5$, $t_{8,\ 0.05} = 1.686$, $p =$ ns). (**e**, **f**) Nucleosome occupancy analysis 3 h after training on selected κB sites of genes encoding for NMDAR (**e**) and AMPAR (**f**). (NMDAR: $n_{\text{No-TR}} = 5$, $n_{\text{sTR}} = 4$, $t_{7,\ 0.05} = 0.7255$, $p = 0.4917$; AMPAR: $n_{\text{No-TR}} = 5$, $n_{\text{sTR}} = 4$, $t_{7,\ 0.05} = 0.8251$, $p = 0.4365$). $^*p < 0.05$. In all cases, values are expressed relative to No-TR

CA3 pyramidal cells (data not shown). The presence in nuclei was confirmed using propidium iodide (PI), and we detected that this nuclear marker co-localizes with the immunolabeling of CamKIIδ (Fig. 5a). In particular, we compared total intensity of CaMKIIδ fluorescent signal inside the nucleus with CaMKIIδ signal outside the nucleus, delimitated by PI staining (see the "Materials and Methods" section). Using this methodology, we found that in all of the analyzed cases, CaMKIIδ signal was higher inside than outside the nucleus (Fig. 5a, right graph), indicating its predominant nuclear location.

In order to study CaMKIIδ protein localization in pyramidal dendrites, we took advantage of Thy1-GFP M transgenic mice (Jackson Laboratory, USA) that express the green

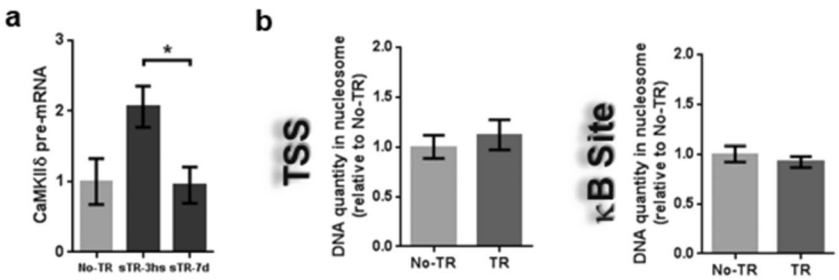

Fig. 4 CaMKIIδ pre-mRNA levels after strong training and nucleosome occupancy changes 3 h after standard training. (**a**) CaMKIIδ pre-mRNA levels different time-points after strong training ($n_{\text{No-TR}} = 4$, $n_{\text{sTR, 3 h}} = 5$, $n_{\text{sTR, 7 days}} = 7$, $F = 4.636$, $p = 0.0302$). (**b**) DNA quantity in nucleosomes 3 h after standard training (TSS $n_{\text{No-TR}} = 7$, $n_{\text{sTR}} = 5$, $t_{10,\ 0.05} = 0.6551$, $p =$ ns; κB $n_{\text{No-TR}} = 7$, $n_{\text{sTR}} = 5$, $t_{10,\ 0.05} = 0.7482$, $p =$ ns). In all cases, values are expressed relative to No-TR

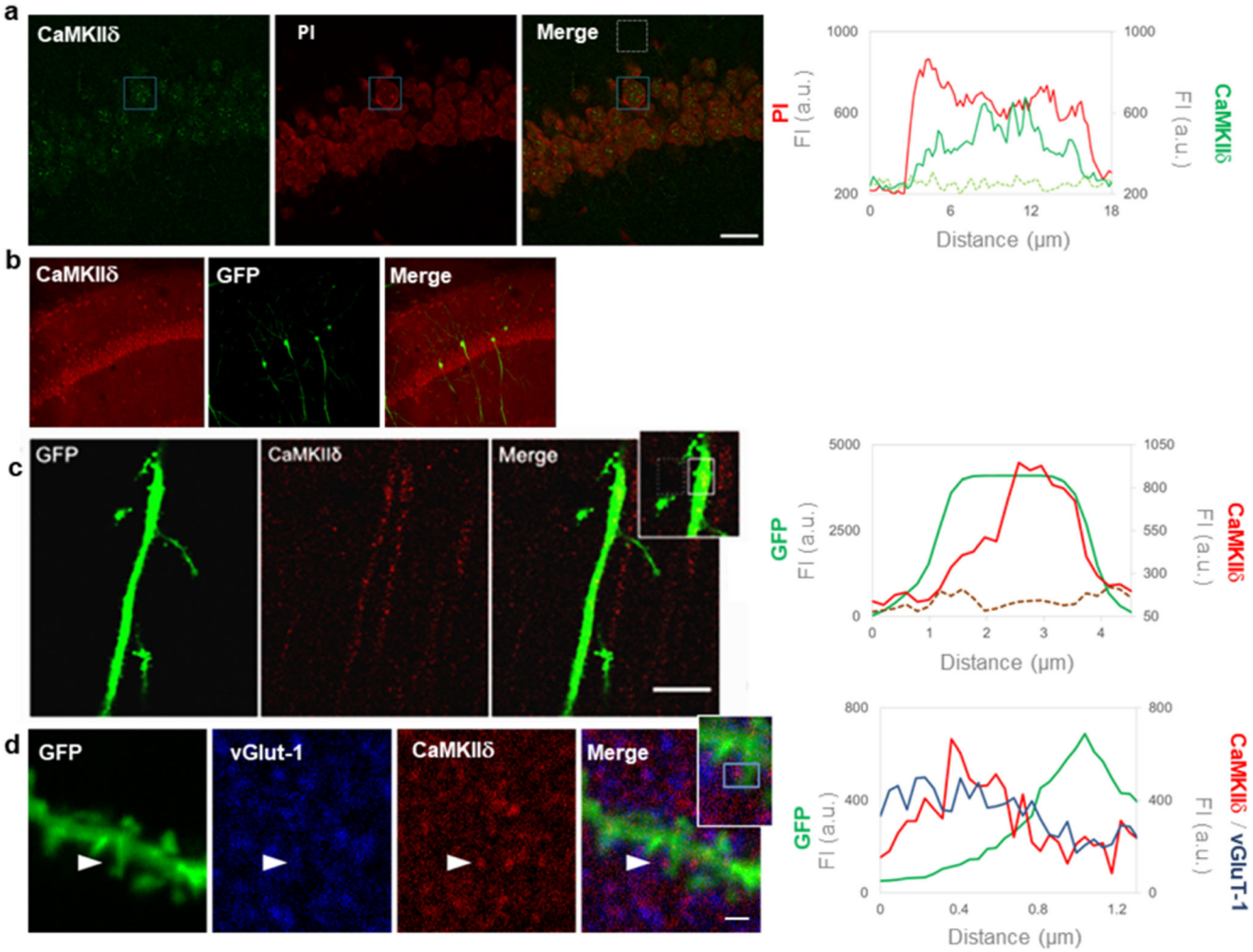

Fig. 5 CaMKIIδ localization in nuclei, dendrites, and pre-synapses of CA1 hippocampal pyramidal neurons. (**a**) Nuclei stained with PI (left), CaMKIIδ immunostaining (middle), and merged image (right) (60 × 1, scale bar = 20 μm). Squares drawn on merged image show an example of the areas employed for the profile analysis plotted on the graph of the right (red line, pI profile inside the solid line square; green line, CaMKIIδ profile inside the solid line square; green dotted line, CaMKIIδ inside the dotted line square). (**b**) GFP labelling of pyramidal neurons on Thy-1 mice (20 × 1, scale bar = 200 μm). (**c**) Dendrites labeled with GFP (left), CaMKIIδ immunostaining (middle), and merged image (right) (yellow indicates CaMKIIδ labelling inside the dendrite) (60 × 1, scale bar = 10 μm). Squares drawn on the inset image show an example of the areas employed for the profile analysis plotted on the graph of the right (green line, GFP profile inside the solid line square; red line, CaMKIIδ profile inside the solid line square; brown dotted line, CaMKIIδ inside the dotted line square). (**d**) Dendrites and spines labeled with GFP (left), vGlut-1 immunostaining (middle left), CaMKIIδ immunostaining (middle right), and merged image (right) (60 × 8, scale bar = 1 μm). Arrow indicates the synapse analysis which is magnified in the inset image to show the analyzed area (solid line square). Emission profiles were plotted on the graph of the right: vGlut-1 in blue indicates the pre-synaptic compartment, GFP (green line) indicates the post-synapsis, and the red line is for CaMKIIδ

fluorescent protein (GFP) in specific subset of dispersed neurons (Fig. 5b), allowing to distinguish dendrites and spine morphology. The co-localization of GFP and the antibody in the same focal planes of confocal images is shown in Fig. 5c,d and was confirmed by densitometric profile analysis (Fig. 5, right panels). We compared the total fluorescence intensity of CaMKIIδ signal inside with that outside the dendrite, delimitated by GFP signal. Using this approach, we found that CaMKIIδ is present in all of the analyzed dendrites.

We also studied CaMKIIδ presence at the synaptic compartments. We found that in most cases, CaMKIIδ signal is localized nearby but not exactly in the post-synaptic density. This observation prompted us to perform immunofluorescence studies using an antibody which binds to the pre-synaptic marker vesicular glutamate transporter-1 (vGlut-1), present at excitatory pre-synaptic terminals. Figure 5d shows a representative example of vGlut-1 and CaMKIIδ immunofluorescence signal in the vicinity of dendritic spines in which it can be seen that CaMKIIδ is present mostly at the pre-synaptic terminal. We further used densitometric profile analysis to assess the presence of CaMKIIδ at the pre- and post- synaptic compartments. CaMKIIδ immunofluorescence signal was higher in the pre-synapse than in the post-synapse, and the fluorescence profile shape fitted very well to that of the

vGlut-1 signal. Using this approach, we found that CaMKIIδ was present in the pre-synaptic terminals of 46% of the studied synapses and in the post-synaptic density in 12% of the studied synapses. In some cases, CaMKIIδ was present at both pre- and post-synaptic compartments.

In conclusion, the immunofluorescence analysis revealed that CaMKIIδ protein is predominantly distributed in nuclei, dendrites, and pre-synaptic terminals.

Discussion

CaMKIIδ function has been largely overlooked in learning and memory processes. In this work, we describe that the sustained expression of CaMKIIδ gene in the hippocampus is specifically necessary for long-lasting forms of memory. In relation with its sustained expression, nucleosome occupancy changes were found here for the first time as epigenetic modifications induced by strong training, for the establishment of a persistent memory. CaMKIIδ gene expression induced by strong training is prolonged at least for 7 days. This is a remarkably persistent molecular mechanism. To our knowledge, most of the training-induced molecular changes previously described occur within some hours after training. An exception to this is the PKMz expression that is proposed as a key mechanism of memory maintenance and whose expression was shown to be increased up to seven days after training in the insular cortex [30] and for one month in the hippocampus [31]. Our present results showing such a prolonged expression of CaMKIIδ gene are consistent with other findings which show that CaMKIIδ mRNA expression in the peripheral neural system is increased seven and even more days after nerve injury [6, 32].

The experiments with ASO infusion showed that CaMKIIδ gene expression during consolidation is not necessary for 1-day memory retention but is required for memory to persist 1 week after training. These results indicate that CaMKIIδ gene is required for processes that warrant enduring memory retention, different from the role proposed to other isoforms of this protein kinase [8]. The increase in CaMKIIδ gene expression during consolidation may be necessary to trigger the maintenance of the nuclear and synaptic changes that occur in this memory phase, and this could explain why decreasing the mRNA levels with the ASO impairs 7-day but not 1-day memory retention. A question that arises at this point is whether CaMKIIδ ASO infusion 2 or 24 h after training is also affecting CaMKIIδ expression at day 7, when NOR performance is impaired. Phosphorothioated oligonucleotides have been reported to remain stable up to 5 h and sometimes 24 h after intrahippocampal injection [33, 34]. Therefore, we expect the ASO to have a direct effect on CaMKIIδ expression within the first 24 h after its administration. However, as shown from our results in Fig. 1b, given that CaMKIIδ expression levels parallel memory retention, we believe that CaMKIId mRNA could also be decreased during the 7-day test. This could be the consequence of a direct interruption of a CaMKIIδ-dependent memory maintenance mechanism around the time of ASO administration and/or because decreasing CaMKIIδ levels blocks some feedforward sustainment of its own expression.

In the present work, the persistent expression of CaMKIIδ gene paralleled the time course of memory retention after strong training. These findings prompted us to evaluate if the prolonged expression is in fact necessary for retention. Effectively, we found that CaMKIIδ gene expression inhibition in the hippocampus at 24 h, when consolidation is supposed to be completed, impaired 7-day memory retention. At this time point, memory is expected to be not sensitive to amnesic treatments [35]. Thus, our data support that CaMKIIδ gene expression at such late phase acts as a mechanism of memory maintenance, the interruption of which caused memory impairment even beyond consolidation.

It is worth mentioning that, while the measures of CaMKIIδ mRNA represent CaMKIIδ expression levels at different time-points after training, the molecular profile of animals that underwent a testing session could not be identical because of the retrieval process.

The sustained expression of CaMKIIδ gene is a remarkable finding that led us to investigate possible control mechanisms involved in such an enduring process. Although an important topic in other fields like cancer research, nucleosome positioning has received little attention in neuroscience, and no data are available on nucleosomal sliding and/or ejection in memory or neural plasticity. In our study, nucleosome occupancy changes were observed at both CaMKIIδ promoter κB and TSS sites, but with quite different dynamics. At the κB site, nucleosome positioning changed only shortly after training. In contrast, changes in nucleosome positioning at TSS were observed during consolidation and also 7 days after training, paralleling CaMKIIδ expression and memory retention. This could be explained by the fact that NF-κB is activated specifically during consolidation, and thus, this is a critical time-point in which the expression of NF-κB-dependent genes, like *camk2d*, is regulated. CaMKIIδ expression after consolidation could be independent of NF-κB activity, and therefore, nucleosome occupancy at the κB site is not affected. In a previous study from the lab, we found that NF-κB binds to the κB site of CaMKIIδ promoter 1 h after object recognition training, suggesting indeed that learning-induced CaMKIIδ expression during the first hours after training is regulated, at least in part, by NF-κB [3]. We also found that, at this same time-point, training induced H3 acetylation at the κB site. This epigenetic modification could be enhancing NF-κB DNA-binding, as histone acetylation is expected to decrease DNA–histone interaction and increase DNA accessibility [36, 37]. In the present work, we found that nucleosome positioning at the κB site

is increased 3 h after NOR training, but it is not affected 1 h after. In general, it has been observed that the presence of a nucleosome in TF binding sites modulates negatively the expression of the gene of interest [19], and in vitro studies have demonstrated this for NF-κB, in particular [38]. Therefore, a plausible interpretation of our recent and previous results is that 1 h after training, nucleosome occupancy changes are not required for NF-κB to bind to its κB site and that 3 h after, the changes observed in nucleosome occupancy take place to regulate NF-κB-dependent gene expression of CaMKIIδ, possibly in a negative manner.

Regarding the nucleosome occupancy changes observed at the TSS site, they are expected to be related to changes in gene expression. At the moment, it is not possible to interfere with nucleosome occupancy specifically at CaMKIIδ gene to study how this affects its gene expression. However, measuring pre-mRNA levels of *camk2d* gene is a good indicator of its expression status. Therefore, based on our results, it is possible that the decrease in nucleosome occupancy found during consolidation accounts for the increase in pre-mRNA and mRNA observed 3 h after training (Figs. 1e and 4a), while the increase observed 7 days after may be inhibiting its pre-mRNA gene expression (Fig. 4a). This interpretation is supported by evidence showing that the presence of a nucleosome in the transcription start site may weaken the binding of the RNA polymerases leading to a decrease in gene expression, while the absence of nucleosome facilitates it [19, 22, 23]. The fact that 7 days after training mRNA but no pre-mRNA levels are still increased compared to control groups could be explained by differential RNA processing and stability of the mature form. Finally, no changes were found 20 days after training at the studied regulatory regions of the gene, when gene expression and memory retention already vanished. Thus, the prolonged changes in this epigenetic mechanism are likely to be associated with the prolonged expression of the gene and the persistence of the memory.

Despite the wide use of NOR in the field of neurobiology, the underlying neural areas supporting this task are under debate. In particular, considerable debate took place on whether the hippocampus plays a significant role in object recognition memory. The experimental results presented here support the participation of the hippocampus. The inhibition of Camk2d expression in hippocampus prevented remote recognition memory retention, whereas the expression of Camk2d in hippocampus is induced after NOR strong training. In the literature, many evidence supports the participation of the hippocampus in recognition memory, and it was proposed that the duration of the sample session is critical for the involvement of hippocampus in this task [39]. In fact, in our experiments using the strong training, we employed an extended sample session.

We found that CaMKIIδ is present in the nucleus of hippocampal pyramidal cells. Previously, CaMKIIδ was found in cerebellar granule cell nuclei [40]. In another physiological process, the cardiac hypertrophy, it was found that nuclear CaMKIIδ induces epigenetic mechanisms that favor gene expression by phosphorylation of histone H3 [41]. In addition, CaMKIIδ phosphorylates and induces nuclear exportation of histone deacetylase 4 (HDAC4), affecting gene transcription [42, 43]. Notably, HDAC4 is one of the HDAC subtypes mostly studied in neural plasticity and memory [44], and its role in this process is evolutionarily conserved [45, 46]. Thus, the increase in CaMKIIδ expression after training might lead to transcription events that allow the maintenance of the memory trace.

We also found CaMKIIδ located in pre-synaptic terminals. Even though strong evidence points out to a crucial role for pre-synaptic CaMKII in synaptic plasticity and neurotransmitter release [47, 48], it has not yet been assessed its specific role in memory and little is known about the presence of each isoform in this compartment. Thus, to the best of our knowledge, these results are the first showing that CaMKIIδ is present at the pre-synaptic terminals. The fact that not all of the excitatory pre-synaptic terminals were CaMKIIδ-positive is an interesting observation that deserves further investigation.

In conclusion, all the findings presented here point to a critical role of a largely overlooked neuronal δ CaMKII isoform in the mechanisms that define the persistence of memory over time.

Materials and Methods

Animals

C57BL/6J male mice, 7–9 weeks old and weighing approximately 25 to 30 g were used for all experiments except for some immunofluorescence studies as indicated in which we used transgenic Thy1 (Tg MJrs Thy1-EGFP/J; http://jaxmice.jax.org/strain/007788.html). Mice were provided by animal facilities of the University of Buenos Aires, Argentina. Animals were housed in groups of four individuals; after cannulation, they were housed individually. Water and mice pellet food were provided ad libitum. Mice were kept under a 12 h light/dark cycle (lights on at 8:00 A.M.) at a temperature of 21–22 °C. Experiments were carried out during the light phase. Experimental procedures were performed in accordance with the FCEN-UBA regulations and the National Institutes of Health (NIH) Guide for the Care and Use of Laboratory Animals (NIH publication 80-23/96), USA. All efforts were made to minimize animal suffering and to reduce the number of animals used.

Training–Testing Apparatus and Behavioral Procedure

The experimental chamber consisted of a plastic box with a transparent lid and white walls (30 × 21.5 × 30 cm); the floor was covered with shavings. The novel object recognition (NOR) procedure has been described in detail before [3]. Briefly, it consisted of two days of mice handling for 3 min, once a day, followed by three days of habituation that involved placing each animal in the experimental chamber for 5 min once a day, with no object presentation. On the following day, mice were trained in the experimental chamber containing two identical objects as indicated in Fig. 1a. The objects used were 100 ml transparent beakers or blue blocks (Rasti® toy), both of similar size. They were allowed to explore the objects for 10 min (standard training) or 15 min (strong training), depending on the experiment. In some cases, a control group (No-TR) was included during this session, in which mice were introduced in the arena for 15 min but without objects. Memory retention was assessed either 1, 7, or 20 days after training on independent experiments. The testing session involved introducing the animals to the experimental chamber and allowing them to explore two different objects (a beaker and a block) for 5 min. One of the objects was identical to those explored during the training session (familiar object) and the other was a different object (novel object). The objects were exposed in the same locations of the chamber as they were in the training session. The location of the novel object was exchanged between the left and the right for different animals to avoid place preference during the evaluation session. Training and testing sessions were filmed with a Logitech web camera model type Tessar 2.0/3.7 2 MP autofocus, which was connected to a computer using the program Logitech Quicktime®. The camera was placed 30 cm above the experimental chamber for later analysis. All the manipulations were performed wearing disposable gloves.

Behavioral Data Analysis

Time spent exploring each object was measured with two stopwatches (one for each object), for both training and testing sessions. The time that mice spent exploring the objects was established as the time during which animal oriented its head towards an object, with his nose 1 cm or less around it. The time that the animal spent above the object was not considered. During training, total time of exploration was determined, and it was also verified that animals had no preference for right or left object (the mean relative time of exploration was not statistically different between objects). During testing session, the relative time of novel object exploration was calculated as the discrimination index: $DI\% = (t_{novel} - t_{familiar}) / (t_{novel} + t_{familiar})$ (× 100%). The mean DI% value was calculated for the different groups of animals. Depending on the number of groups, Student's *t* test or one-way ANOVA was used, using a per comparison error rate (α) of 0.05 for statistical comparisons between groups. Total times of exploration for each group in training and testing sessions were compared in all of the experiments to verify that there were no differences between groups in this parameter. Animals showing low exploration times (below two standard deviations) were excluded from the experiments (approximately 1% of the animals). Mean exploration time in the testing session for behavioral experiments was No-TR = (7.6 ± 0.5), TR (10 min) = (6.7 ± 0.5) s and in sTR (15 min) = (6.6 ± 0.5) s, one-way ANOVA (no significant variability was found between different experiments, $F_{2,44} = 1.12$, p = ns). No significant differences were found between exploration time of injected and non-injected animals.

Surgery and Drug Infusion

Under deep anesthesia (70 μl of ketamine 5% *w*/*v* and 20 μl of xylazine at 20 mg/ml), mice were bilaterally implanted with 23-gauge guide cannulae 1 mm dorsal to their dorsal hippocampi at coordinates of anterior, − 1.9; lateral, ± 1.2; and ventral, 1.2, in accordance with the atlas of Paxinos and Franklin [49]. Guide cannulae were fixed to the skulls with dental acrylic containing calcium hydroxide. Handling for NOR task was performed three days after surgery to ensure animal recovery. The injection device consisted of a 30-gauge cannula connected to a 5 μl Hamilton syringe. Initially, the infusion device was filled with distilled water, and a small air bubble was sucked into the injection cannula, followed by the injection solution. The air bubble allowed for visual inspection of the injection progress. The injection cannula was inserted into the guide cannula with its tip extending beyond the guide by 1 mm so as to reach the dorsal hippocampus. Injections were administered across a 30 s time period. Injection cannula was removed after 60 s to avoid reflux and to allow the diffusion of drugs. The volume of each intrahippocampal infusion was 1 μl/side. Different injection devices were used for drug and vehicle. The injections were performed 2 or 24 h after the training session. After behavioral procedures, animals were injected with black ink and were decapitated. Brains were placed in 4% paraformaldehyde for 1 day, followed by 30% sucrose for an additional 24 h. To verify cannula placement, frozen brains were sliced using a cryostat and analyzed under microscope. The deepest position of the needle was superimposed on serial coronal maps. Only data from animals with cannulae located in the intended sites were included in the analysis.

Drugs

An oligodeoxinucleotide (ODN) of 20 bp was designed complementary (antisense) to the *camk2d* mRNA, with the sequence 5′ CTTTCCGAGCTCCTCAAAGA 3′. A scrambled sequence of the same bases was used as a control ODN, with

the sequence 5′ CATTCACTCACGTTACGAGC 3′. The thermodynamic stability of the antisense ODN was analyzed using the online tool OligoAnalyzer 3.1 (Integrated DNA technologies). The specificity of the scrambled ODN with any mRNA sequence was discarded after analysis with the online tool "Nucleotide Blast" (NIH, USA). The three first and last bases of each ODN were phosphorothioated. Each ODN was re-suspended in sterile saline solution at a final concentration of 1 nmol/μl and injected 1 nmol per hippocampus.

RNA Extraction and Gene Expression Analysis

Mice were killed by cervical dislocation 3 h, 1 day, 7 days, and 20 days after training as indicated. Brains were rapidly removed, and both hippocampi were dissected. Total RNA was extracted using TRIzol LS Reagent (Invitrogen, Life Technologies). Each hippocampus was placed in 1 ml of TRIzol, and tissue was homogenized with 15 strokes in a glass Dounce homogenizer, type A pestle. RNA extraction was performed as indicated by the TRIzol manufacturer. A total of 5 μg of RNA was used for retro-transcription reaction. For pre-mRNA retro-transcription instead of oligodT, we used the following specific probes that fall in introns of *camk2d* and *b actin* genes, respectively: 5′-TTAGTGCAAAGAAG GATAGC-3′ and 5′-AGACCTACTGTGCATCTACT-3′. The cDNA obtained was subjected to real-time PCR in 25 μl of reaction buffer containing 0.8 mM dNTPs, 2.5 units of Taq DNA polymerase (Invitrogen), and 10 μM of the primers specific for mouse *βactin* or the *Camk2d* mRNA, designed as follows:

βactin mRNA
Forward: 5′-TCCTTCCTGCCTATGGAATC-3′,
Reverse: 5′-ACTCATCGTACTCCTGCTTG-3′.
βactin pre-mRNA
Forward: 5′-GGCTGTATTCCCCTCCATCG-3′,
Reverse: 5′-TCTTAGCACCGGCATCGATC-3′.
Camk2d mRNA
Forward: 5′-TTCGGACACGGAAAGTGAGG-3′,
Reverse: 5′-TTCTCACCACTGAGAACGCC-3′.
Camk2d pre-mRNA
Forward: 5′-GGTTCACCGACGAGTATCAG-3′,
Reverse: 5′-CCCGCAGGCTCTCTATCC-3′.

For both genes, PCR reactions were performed at 95 °C for 15 s, 60 °C for 20 s, and 72 °C for 20 s, for a total of 39 cycles. To calculate the efficiency of the reaction and confirm that the sample concentration was within the quantitative PCR region, a seven-point standard curve, prepared from serial dilutions of a mixture containing the original cDNA of all samples, was also amplified for each primer pair. Finally, the cumulative fluorescence for each amplicon of each group of animals was normalized to control No-TR group.

Nucleosome Occupancy Analysis

Nucleosomal DNA Extraction

Mice were sacrificed by cervical dislocation at different intervals after a NOR training. Their brains were removed quickly, and both hippocampi were dissected and stored at − 80 °C. For isolation of nuclei, hippocampal tissue was homogenized with 3 ml of buffer 1 (60 mM KCl, 0.3 M sucrose, 15 mM NaCl, 5 mM $MgCl_2$, 0.1 mM EGTA, 15 mM Tris–HCl, pH 7.5, 0.5 mM DTT, 0.1 mM PMSF, and 3.6 ng/ml aprotinin) using a Teflon-glass homogenizer (15 strokes). Then, samples were centrifuged (1000 rpm, 10 min, 4 °C) and resuspended in 1 ml of buffer 1 and 1 ml of buffer 2 (Idem to buffer 1 but with 0.4% *v*/*v* of IGEPAL CA-630); these steps induce lysis of the cell membrane and release the nuclei of neurons. The cores were then separated from cytosolic components by centrifugation in sucrose cushion using buffer 3 (Idem to buffer 1 but with 1.2 M sucrose). Nuclei were collected from the bottom of the tube, resuspended in 500 μl of digestion buffer, and incubated with micrococcal nuclease enzyme (MNase digests DNA unbound to nucleosome). Nucleosomal DNA was isolated from nucleosomes by phenol–chloroform–isoamyl alcohol extraction. Finally, the DNA was precipitated from the aqueous phase using ethanol, glycogen, and 3 M sodium acetate, and resuspended in 30 μl of water Milli-Q. Since the study requires that MNase digestion is complete, i.e., that digests the entire DNA to stay mononuclesomal, it was verified that the recovered DNA fragments have about 147 pb.

Nucleosomal DNA Quantification.

DNA was subjected to qPCR using specific primers for NF-κB binding site and transcription start site (TSS) at *camk2d* promoter, fibronectin intergenic region (housekeeping), *Gria1* promoter (codes for Glu-A1 AMPAR subunit), or *Grin2a* promoter (codes for NR2Aε1 NMDAR subunit), as indicated

Camk2d TSS
Forward: 5′-CGGGGAGAGGAGGGAGGAG-3′,
Reverse: 5′-CCGCAAGGCTGGGAACCC-3′.
Camk2d κB site
Forward: 5′-GCACTTTTGGGTTTCATTATGTTAG-3′,
Reverse: 5′-CGTCTTCGCCCTTCTCTCC-3′.
Fibronectin intergenic region
BDChFNInterF: 5′-CAGTCCTAATCAGCAAGCAG AAG-3′,
BDChFNInterR: 5′-AAGCACCCATAAAGCAGTTA ATTG-3′.
Gria1 κB site
Forward: 5′-TATGCCTTTCTCACAGTCTTTC-3′,
Reverse: 5′-ATTATTCCTACAACTAATTCCCAAG-3′.

Grin2a κB site
Forward: 5′-TGCTGAGGTCATCATCCC-3′,
Reverse: 5′-TAATATACTTCTGGCTTCAATGC-3′.

These primers were designed de novo using the Beacon Designer software. For each pair of primers, the specificity of PCR reaction was verified by running PCR products on an agarose gel stained with ethidium bromide products and confirming that the size of the amplified product coincided with the expected one.

Fibronectin gene contains nucleosomes that should not be affected by behavioral experience. Therefore, for each sample, a fibronectin PCR reaction was performed in parallel to the promoter site of interest and each value was normalized to that of fibronectin.

After normalizing the results of each sample to the values of fibronectin, the average value for each group relative to the group average No-TR in each case was calculated.

Immunofluorescence Analysis

Naïve C57BL/6 or transgenic Thy1 (Tg MJrs Thy1-EGFP/J http: //jaxmice.jax.org/strain/007788.html) were used, as indicated. Mice were deeply anesthetized with ketamine/xylazine and perfused transcardially with saline followed by 4% paraformaldehyde (PFA) in 0.1 M phosphate buffer (PB). Brains were removed and post-fixed for 6 h in 4% PFA in 0.1 M PB (4 °C) and transferred to 30% sucrose in PBS (4 °C, ON). Brains were cut in 40 μm coronal sections using a cryostat.

Incubations

Brain sections were permeabilized with 1% Triton X-100 PBS for 5 min at room temperature (RT), followed by three incubations in 0.3% Triton X-100 PBS (washing solution). Next, sections were blocked in 2.5% normal goat serum (50197Z; Invitrogen, diluted in 0.3% Triton X-100 PBS) for 1 h at RT and then incubated with primary antibody (4 °C, ON). After three passages on washing solution, sections were incubated with secondary antibody for 1.5 h at RT. Next, sections were washed three times with PBS and mounted on glass holder using a mounting medium containing propidium iodide (PI) for nuclear localization studies (F5932, Sigma-Aldrich) or Vectashield mounting medium (H-1000; Vector Laboratories ®) in the other cases. As a control, the same incubation protocol was performed in parallel on fresh slices from the same animal but in the absence of primary antibody. For the analysis at synapses in which two primary antibodies were used (anti-CaMKIIδ and anti-v-Glut-1), ON incubation with each primary antibody was performed separately on consecutive days, and no cross-binding between primary and secondary antibodies was corroborated using control sections incubated in the absence of one of the primary antibodies.

Antibodies

Primary antibodies: anti-CaMKIIδ (rabbit), cat. no. A010-56AP, Badrilla® and anti-VGLUT-1 (mouse), cat. no. AB5905, EMD Millipore Corporation. Both antibodies were used at a concentration 1:200 diluted in 2.5% normal goat serum 0.3% Triton X-100 PBS. Secondary antibodies: goat anti-rabbit Alexa Fluor 488 and Alexa Fluor 594 (1:250 in 2.5% normal goat serum, Thermo Fisher Scientific) and donkey anti-mouse conjugated with cytochrome5, ab6563, Abcam (1:250 in 3% BSA in PBS).

Confocal Microscopy

For each experimental condition, two sections from two different animals were viewed in a confocal microscope Olympus FV300. Image capture was performed using the microscope software, and in all cases, it was carried out sequentially: images for each of the fluorescent components were taken separately, one immediately after the other. For studies on nuclear localization, helium–neon laser (594 nm) was first used to capture propidium iodide emission and then the argon laser (488 nm) to analyze CaMKIIδ. For dendrite study, the helium–neon laser (594 nm) was first used to visualize CaMKIIδ and then the argon laser (488 nm) to visualize GFP. For the study at synapses, the helium–neon laser (633) was first used to visualize VGLUT-1 emission and then the helium–neon laser (594 nm) to visualize CaMKIIδ and finally laser argon (488 nm) to visualize GFP. For each study and for each fluorescent signal to be analyzed, a first quick visualization of the slices was performed to define the optimal optical parameters (laser intensity, offset, photomultiplier, gain, and confocal aperture) which were kept fixed throughout the entire imaging session. Filters were chosen appropriately for each case. The objective lens used was UPLFL20× (confocal aperture 1.0) and PLAPO60× (confocal aperture 2.0). For every picture taken (in each confocal plane), a scan was performed in duplicate and a Kalman filter to reduce noise background was applied. Images were processed using ImageJ software 1.48 V.

Nuclear Localization Studies

Ten neurons were randomly chosen from CA1 region of the hippocampus. A rectangle was drawn above the soma of each neuron. PI staining was used as nuclear marker, and CaMKIIδ fluorescence intensity was assessed on the pixels that overlap with PI staining (“inside PI”) and outside PI label but inside the rectangle (“outside PI”). Then, this procedure was repeated locating the rectangle in a nearby region where nuclei were absent and fluorescence intensity was assessed on an equivalent number of pixels used for “inside PI” and “outside PI,” respectively. These second values were measured to

standardize the fluorescence values obtained from the rectangle located above a neuron and make this total fluorescence intensity independent of the number of pixels used. Fluorescence intensity measures for the total amount of pixels in each case were used to calculate an intensity ratio (IR) of CaMKIIδ fluorescence inside nucleus relative to outside:

$$IR = \frac{\left(TI_{\text{inside PI}}/TI_{\text{equivalent i}}\right)}{\left(TI_{\text{outside PI}}/TI_{\text{equivalent o}}\right)}$$

where $TI_{\text{inside PI}}$ is total intensity (TI) in the pixels present inside PI labelling, $TI_{\text{equivalent i}}$ is TI in the same number of pixels in the rectangle located where nuclei were absent, $TI_{\text{outside PI}}$ is for the total number of pixels that fell outside PI staining but inside the rectangle, and $TI_{\text{equivalent o}}$ is TI in the same number of pixels but on the rectangle located where no nucleus were present. This ratio was obtained for different nuclei across different slices and an average value was calculated. This value was used to construct a confidence interval (CI, 95%). The CI obtained was ($t_{0.05/2,\ 9} = 2.262$): [1.20–1.47]. A CI greater than 1 indicates that CaMKIIδ fluorescence intensity inside the nucleus is significantly higher than outside, indicating its presence in the nucleus using a correct and equivalent focal plane. Next, we considered to be nuclear-positive those neurons whose intensity ration was above 1 even after subtracting 2 standard deviations.

Dendrite Localization Studies

The study was conducted on 13 main dendrites, i.e., those from which were born branches to smaller dendrites. This was so because in dendrites that branched to spines it was very difficult to separate the mark of the spine from that of the dendrite itself. Main dendrites are bulkier and thorns present in them are lower. Having identified the dendrite, three different regions were chosen along this, and GFP and CaMKIIδ fluorescence profiles were analyzed. The profile of GFP fluorescence was used to delineate the edges of the dendrite in each case. Total CaMKIIδ fluorescence intensity was then calculated for all pixels that fell inside the dendrite and outside but inside the rectangle, respectively. The same procedure was repeated for a rectangle positioned at a nearby place that contained no dendrites, and fluorescence intensity was assessed on a same number of pixels (similar to the analysis for nuclear studies). Once again, we calculated the IR of CaMKIIδ inside and outside the dendrite using the same formula than described previously. This procedure was repeated for three different regions along the same dendrite. In many cases, these regions were in different planes in the z axis. Then, an average from these three IR values was calculated and used to build a CI confidence interval ($t_{0.05/2,\ 2} = 3.182$). If the CI for each dendrite was above 1, we considered it to be positive for CaMKIIδ.

Synaptic Localization Studies

First, we observed GFP and VGLUT-1 fluorescence profiles for different synapses, and we considered for the analysis 27 from two animals in which the pre- and post-synaptic compartments were clearly differentiated. Similarly to what was done previously, a rectangle containing the synapse was drawn and the corresponding fluorescence profile was plotted. VGLUT-1 and GFP profiles were used to delimit pre- and post-synaptic compartments and CaMKIIδ fluorescence intensity was obtained for each region. We used the same rectangle to measure fluorescence intensity on a nearby region and calculated the IR as before. Since in many cases, the area of the pre- and post-synaptic compartments was not equivalent, IR values were multiplied by a factor f that corrected the fluorescence intensity based on the relative number of pixels in both compartments. Thus, the final calculation was as follows: $\text{IR} = \text{IR}_{\text{PRE/POST}} \cdot f$, where $f = n_{\text{post}} / n_{\text{pre}}$ and n is the number of pixels on which the fluorescence intensity for each compartment was measured. Then, to decide whether CaMKIIδ was mostly present in pre, post, or equally on both, the following criteria were adopted: if IR was 1.0, it was considered to be found equally in both. If it was equal or greater than 1.1, it was predominantly in pre, and if equal or lesser than 0.9, it was found predominantly in post.

Statistical Analysis

Student's t test was used when comparisons were carried out between two groups. In experiments with more than two groups, a one-way ANOVA was performed, followed by Duncan's post-hoc test, except otherwise indicated. The assumptions of normality and homoscedasticity for each case were evaluated using the Shapiro–Wilk's statistic and Brown–Forsythe test, respectively. In some cases, data from experiments in which amount of mRNA was evaluated showed minor deviations to normality; however, since the statistical ANOVA is robust to small deviations in this case, it was considered valid to use this statistical model to analyze these data [50]. Statistical analyses were performed with GraphPad Prism or InfoStat software. Confidence intervals for immunofluorescence studies were constructed using the following formula: $(X - EEt_{\alpha/2,\ n-1};\ X + EEt_{\alpha/2,\ n-1})$ where x is the average of the values, EE is standard error, and t the t value obtained from the corresponding tables assuming normal distribution. Data was presented as mean ± S.E.M.

Acknowledgments We thank Dr. María Eugenia Pedreira and Dr. Damian Refojo for helpful comments on the manuscript. This work was supported by research grants from the National Agency of Scientific and Technological Promotion of Argentina (ANPCyT) PICT2369, National Council of Research (CONICET) PIP5466, and University of Buenos Aires grant X198.

References

1. Zovkic IB, Guzman-Karlsson MC, Sweatt JD (2013) Epigenetic regulation of memory formation and maintenance. Learn Mem 20(2):61–74
2. Miller CA, Gavin CF, White JA, Parrish RR, Honasoge A, Yancey CR, Rivera IM, Rubio MD et al (2010) Cortical DNA methylation maintains remote memory. Nat Neurosci 13(6):664–666
3. Federman N, de la Fuente V, Zalcman G, Corbi N, Onori A, Passananti C, Romano A (2013) Nuclear factor κB-dependent histone acetylation is specifically involved in persistent forms of memory. J Neurosci 33(17):7603–7614
4. Kwapis JL, Helmstetter FJ (2014) Does PKM(zeta) maintain memory? Brain Res Bull 105:36–45
5. Tsokas P, Hsieh C, Yao Y, Lesburguères E, Wallace EJC, Tcherepanov A, Jothianandan D, Hartley BR et al (2016) Compensation for PKMζ in long-term potentiation and spatial long-term memory in mutant mice. eLife 5
6. Bangaru MLY, Meng J, Kaiser DJ, Yu H, Fischer G, Hogan QH, Hudmon A (2015) Differential expression of CaMKII isoforms and overall kinase activity in rat dorsal root ganglia after injury. Neuroscience 300:116–127
7. Lisman J, Schulman H, Cline H (2002) The molecular basis of CaMKII function in synaptic and behavioural memory. Nat Rev Neurosci 3(3):175–190
8. Lucchesi W, Mizuno K, Giese KP (2011) Novel insights into CaMKII function and regulation during memory formation. Brain Res Bull 85(1–2):2–8
9. Irvine EE, von Hertzen LSJ, Plattner F, Giese KP (2006) alphaCaMKII autophosphorylation: a fast track to memory. Trends Neurosci 29(8):459–465
10. Bachstetter AD, Webster SJ, Tu T, Goulding DS, Haiech J, Watterson DM, van Eldik LJ (2014) "Generation and behavior characterization of CaMKIIβ knockout mice," PLoS One, vol. 9, no. 8.
11. Sirri A, Bianchi V, Pelizzola M, Mayhaus M, Ricciardi-Castagnoli P, Toniolo D, D'Adamo P (2010) Temporal gene expression profile of the hippocampus following trace fear conditioning. Brain Res 1308:14–23
12. Jarome TJ, Thomas JS, Lubin FD (2014) The epigenetic basis of memory formation and storage. Prog Mol Biol Transl Sci 128:1–27
13. Zovkic IB, Paulukaitis BS, Day JJ, Etikala DM, Sweatt JD (2014) Histone H2A.Z subunit exchange controls consolidation of recent and remote memory. Nature 515(7528):582–586
14. Maze I, Wenderski W, Noh KM, Bagot RC, Tzavaras N, Purushothaman I, Elsässer SJ, Guo Y et al (2015) Critical role of histone turnover in neuronal transcription and plasticity. Neuron 87(1):77–94
15. Vogel-Ciernia A, Matheos DP, Barrett RM, Kramár EA, Azzawi S, Chen Y, Magnan CN, Zeller M et al (2013) The neuron-specific chromatin regulatory subunit BAF53b is necessary for synaptic plasticity and memory. Nat Neurosci 16(5):552–561
16. Vogel-Ciernia A, Wood MA (2014) Neuron-specific chromatin remodeling: a missing link in epigenetic mechanisms underlying synaptic plasticity, memory and intellectual disability disorders. Neuropharmacology 80:18–27
17. Hemstedt TJ, Lattal KM, Wood MA (2017) Reconsolidation and extinction: using epigenetic signatures to challenge conventional wisdom. Neurobiol Learn Mem 142:55–65
18. López AJ, Wood MA (2015) Role of nucleosome remodeling in neurodevelopmental and intellectual disability disorders. Front Behav Neurosci 9:100
19. Bai L, Morozov AV (2010) Gene regulation by nucleosome positioning. Trends Genet 26(11):476–483
20. McGaugh JL (2000) Memory—a century of consolidation. Science 287(5451):248–251
21. Neidl R, Schneider A, Bousiges O, Majchrzak M, Barbelivien A, de Vasconcelos AP, Dorgans K, Doussau F et al (2016) Late-life environmental enrichment induces acetylation events and nuclear factor κB-dependent regulations in the hippocampus of aged rats showing improved plasticity and learning. J Neurosci 36(15):4351–4361
22. Ponts N, Harris EY, Lonardi S, Le Roch KG (2011) Nucleosome occupancy at transcription start sites in the human malaria parasite: a hard-wired evolution of virulence? Infect Genet Evol 11(4):716–724
23. Tirosh I, Barkai N (2008) Two strategies for gene regulation by promoter nucleosomes. Genome Res 18(7):1084–1091
24. Kessels HW, Malinow R (2009) Synaptic AMPA receptor plasticity and behavior. Neuron 61(3):340–350
25. Morris RGM (2013) NMDA receptors and memory encoding. Neuropharmacology 74:32–40
26. Shen K, Teruel MN, Subramanian K, Meyer T (1998) CaMKIIbeta functions as an F-actin targeting module that localizes CaMKIIalpha/beta heterooligomers to dendritic spines. Neuron 21(3):593–606
27. Miller S, Yasuda M, Coats JK, Jones Y, Martone ME, Mayford M (2002) Disruption of dendritic translation of CaMKIIalpha impairs stabilization of synaptic plasticity and memory consolidation. Neuron 36(3):507–519
28. Mishra S, Gray CBB, Miyamoto S, Bers DM, Brown JH (2011) Location matters: clarifying the concept of nuclear and cytosolic CaMKII subtypes. Circ Res 109(12):1354–1362
29. Ma H, Li B, Tsien RW (2015) Distinct roles of multiple isoforms of CaMKII in signaling to the nucleus. Biochim Biophys Acta 1853(9):1953–1957
30. Shema R, Haramati S, Ron S, Hazvi S, Chen A, Sacktor TC, Dudai Y (2011) Enhancement of consolidated long-term memory by overexpression of protein kinase Mζ in the neocortex. Science 331(6021):1207–1210
31. Hsieh C et al. (2016) Persistent increased PKMζ in long-term and remote spatial memory. Neurobiol Learn Mem
32. Xiao H-S, Huang QH, Zhang FX, Bao L, Lu YJ, Guo C, Yang L, Huang WJ et al (2002) Identification of gene expression profile of dorsal root ganglion in the rat peripheral axotomy model of neuropathic pain. Proc Natl Acad Sci U S A 99(12):8360–8365
33. Katche C, Bekinschtein P, Slipczuk L, Goldin A, Izquierdo IA, Cammarota M, Medina JH (2010) Delayed wave of c-Fos expression in the dorsal hippocampus involved specifically in persistence of long-term memory storage. Proc Natl Acad Sci U S A 107(1):349–354
34. Yaida Y, Nowak TS (1995) Distribution of phosphodiester and phosphorothioate oligonucleotides in rat brain after intraventricular and intrahippocampal administration determined by in situ hybridization. Regul Pept 59(2):193–199
35. Shema R, Sacktor TC, Dudai Y (2007) Rapid erasure of long-term memory associations in the cortex by an inhibitor of PKM zeta. Science 317(5840):951–953
36. Quivy V, Van Lint C (2004) Regulation at multiple levels of NF-κB-mediated transactivation by protein acetylation. Biochem Pharmacol 68(6):1221–1229
37. Kim S, Kaang B-K (2017) Epigenetic regulation and chromatin remodeling in learning and memory. Exp Mol Med 49(1):e281
38. Lone IN, Shukla MS, Charles Richard JL, Peshev ZY, Dimitrov S, Angelov D (2013) Binding of NF-κB to nucleosomes: effect of translational positioning, nucleosome remodeling and linker histone H1. PLoS Genet 9(9):e1003830
39. Cohen SJ, Stackman RW (2015) Assessing rodent hippocampal involvement in the novel object recognition task. A review. Behav Brain Res 285:105–117

40. Takeuchi Y, Yamamoto H, Matsumoto K, Kimura T, Katsuragi S, Miyakawa T, Miyamoto E (1999) Nuclear localization of the delta subunit of Ca^{2+}/calmodulin-dependent protein kinase II in rat cerebellar granule cells. J Neurochem 72(2):815–825
41. Awad S, al-Haffar KMA, Marashly Q, Quijada P, Kunhi M, al-Yacoub N, Wade FS, Mohammed SF et al (2015) Control of histone H3 phosphorylation by CaMKIIδ in response to haemodynamic cardiac stress. J Pathol 235(4):606–618
42. Little GH, Bai Y, Williams T, Poizat C (2007) Nuclear calcium/calmodulin-dependent protein kinase IIdelta preferentially transmits signals to histone deacetylase 4 in cardiac cells. J Biol Chem 282(10):7219–7231
43. Zhang T, Kohlhaas M, Backs J, Mishra S, Phillips W, Dybkova N, Chang S, Ling H et al (2007) CaMKIIdelta isoforms differentially affect calcium handling but similarly regulate HDAC/MEF2 transcriptional responses. J Biol Chem 282(48):35078–35087
44. Sando R, Gounko N, Pieraut S, Liao L, Yates J, Maximov A (2012) HDAC4 governs a transcriptional program essential for synaptic plasticity and memory. Cell 151(4):821–834
45. Wang W-H et al (2011) Intracellular trafficking of histone deacetylase 4 regulates long-term memory formation. Anat Rec 294(6):1025–1034
46. Fitzsimons HL, Schwartz S, Given FM, Scott MJ (2013) The histone deacetylase HDAC4 regulates long-term memory in Drosophila. PLoS One 8(12):e83903
47. Ninan I, Arancio O (2004) Presynaptic CaMKII is necessary for synaptic plasticity in cultured hippocampal neurons. Neuron 42(1):129–141
48. Lu F-M, Hawkins RD (2006) Presynaptic and postsynaptic Ca^{2+} and CamKII contribute to long-term potentiation at synapses between individual CA3 neurons. Proc Natl Acad Sci U S A 103(11):4264–4269
49. Paxinos G and Franklin KBJ (2004) The mouse brain in stereotaxic coordinates. Gulf Professional Publishing
50. Kirk RE (2012) Experimental design: procedures for the behavioral sciences, 4th edn. SAGE Publications, Inc, Thousand Oaks